Mendeleev Communications

Focus Article, *Mendeleev Commun.*, 2025, **35**, 367–375

Development of heat-robust and heat-resistant refractory high-entropy alloys: a review

Nina I. Ilinykh, Ilya A. Balyakin, Boris R. Gelchinski and Andrey A. Rempel*

Vatolin Institute of Metallurgy, Ural Branch of the Russian Academy of Sciences, 620016 Ekaterinburg, Russian Federation. E-mail: rempel.imet@mail.ru

DOI: 10.71267/mencom.7742

In this brief review, we consider high-entropy alloys (HEAs) based on refractory metals from the perspectives of their synthesis, composition, properties and applications. We present the results of predicting the element composition of HEAs with the highest melting points, high-temperature strength and heat resistance, as well as an analysis of the atomic structure and physicochemical properties of the synthesized HEAs.

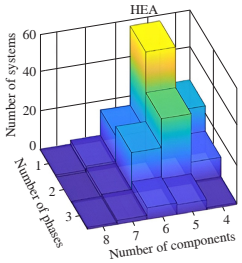

Keywords: high-entropy alloys, HEAs, refractory alloys, heat-robust alloys, heat-resistant alloys.

Introduction

This paper provides a brief review of the advances in the development of heat-robust and heat-resistant refractory alloys characterized by high values of oxidation resistance, mechanical strength, thermal stability, fracture toughness, corrosion resistance, fatigue strength and creep resistance at temperatures exceeding 600 °C under specific loads for prolonged periods.

The development of superalloys, *i.e.* materials distinguished by high heat resistance and high-temperature strength, began in the 1930s in the United States, driven by the demand for novel materials for aircraft turbine engines. In the 1940s, this process was further stimulated by increasing requirements for gas turbine efficiency and later, in the early 1950s, by space-based nuclear reactor programs.[1]

At present, superalloys find widespread application across various industries, including aerospace, nuclear reactors, metallurgy, gas turbine technology, petrochemistry, automotive manufacturing, glass production, medical instruments and other fields. Heat-resistant alloys traditionally used in industry can be classified into three main categories depending on their primary

Nina I. Ilinykh received her PhD in Physical Chemistry from the Institute of Metallurgy of the Ural Branch of the Russian Academy of Sciences (IMET UB RAS) in 1999. Since 2004, she has worked as an associate professor at the Ural Technical Institute of Communications and Informatics. She is currently a senior researcher at IMET UB RAS. Her current research interests include thermodynamic modeling of equilibrium characteristics and composition of complex heterogeneous systems such as solid and liquid metals, oxide and salt solutions, as well as HEAs, using various computational models.

Ilya A. Balyakin graduated from the Ural Federal University (UrFU) with a Master's degree in 2018. In 2023, he earned his Candidate of Sciences degree (PhD equivalent) in Condensed Matter Physics. He conducted his scientific activities at UrFU and IMET UB RAS. Currently, he is a researcher and head of the Laboratory of High-Entropy Alloys at IMET UB RAS, as well as a senior researcher at the Scientific and Educational Center 'Nanomaterials and Nanotechnologies' at UrFU. His scientific interests are focused on neural network molecular dynamics of multicomponent disordered systems.

Boris R. Gelchinski, having received a diploma of mechanical engineer from UrFU in 1970, joined IMET UB RAS as a junior research fellow in 1972. In 1989, he defended his dissertation for the academic degree of Doctor of Physical and Mathematical Sciences in the specialty of Physical Chemistry. His scientific activity is devoted to the study of the structure and properties of metallurgical melts, metal nanopowders, the research into interparticle interaction in metal systems and its relationship with the microscopic structure of liquid metals, revealed by synchrotron radiation and particle scattering methods, as well as computer simulation of the electronic and atomic structure of liquid metals.

Andrey A. Rempel graduated from UrFU in 1981 with a diploma in Experimental Nuclear Physics. He then became a junior researcher at the Institute of Solid State Chemistry of UB RAS and received his PhD degree in Physical Chemistry in 1984 there. In 1992–1998, he was a postdoctoral AvH fellow in the solid state physics group of Prof. Dr. H.-E. Schaefer (Stuttgart University, Germany). In 1997, he earned his Dr. Sci. (Habilitation) degree in Physical Chemistry, in 2007 he received the title of Professor, and in 2019 he was elected an Academician of RAS. His main research interests are high-entropy transition metal alloys and their compounds with carbon and oxygen for various applications.

metal matrix: nickel-based, cobalt-based and iron-based alloys.[2–11]

Detailed reviews of superalloys such as Inconel, Nimonic, Hastelloy, Waspaloy and others are presented by Akca *et al.*[2] and Kollová *et al.*[3] The properties and applications of heat-resistant alloys are described, and the issues on processing of heat-resistant alloys, the study of their microstructure and mechanical properties and the processing of scrap of nickel-based heat-resistant alloys are considered. The most famous companies engaged in the processing of scrap of heat-resistant alloys are presented, including Greystone Alloys (Houston, USA), specializing in the processing of scrap of such metals and alloys as Inconel 625, Inconel 718, Hastelloy C, spray powders, tantalum, Haynes, molybdenum, Monel, tool steel and zirconium; Monico Alloys (Rancho Dominicas, near Los Angeles, USA), which recycles high-purity metal and heat-resistant alloy (Hastelloy, Haynes, Inconel, Monel, Rene and Waspaloy) scrap; and Umicore (with international presence in refineries in Belgium, the USA, the Philippines and China), which uses environmentally responsible and commercially attractive methods to recycle scrap and waste containing cobalt, nickel–rhenium and tantalum.

Heat-resistant nickel-based alloys, which demonstrate a unique combination of mechanical and physical properties at temperatures up to 1150 °C,[4] are the main structural material for high-temperature applications. These superalloys have a complex chemical composition, comprising up to 10–12 components. Iron in these alloys is usually present as an impurity, although there are a number of grades containing up to 30% or more iron. Alloying with chromium (15–20%) provides resistance to high-temperature corrosion. Molybdenum and tungsten, both in solid solution and in carbides, increase the heat resistance of the alloy. Aluminum and titanium with nickel form the γ′-phase $Ni_3(Al,Ti)$, which is the main hardening agent. Cobalt is introduced into nickel alloys to reduce the energy of packing defects and intensify dispersion hardening due to the release of the γ′-phase.

In nickel alloys, after quenching or diffusion annealing and subsequent aging, dispersion hardening occurs with the formation of an intermetallic γ′-phase, which makes a decisive contribution to hardening. The strength of the γ′-phase increases with increasing temperature, while its ductility prevents it from becoming a source of fracture. The heating temperature during quenching and the temperature of diffusion annealing are approximately equal and are usually around 1100–1300 °C. Exposure to high temperatures leads to the dissolution of intermetallic phases with the formation of a homogeneous solid solution with low hardness and obtaining the required grain size. One- or two-stage aging is carried out at temperatures of 700–950 °C. The creep resistance of nickel alloys depends on the morphology of the separated intermetallides and their volume fraction, namely, the finer the separations and the smaller the distance between them, the higher the creep resistance.

The homologous operating temperatures of nickel superalloys are higher than those of other alloying systems, and their share in high-performance engines exceeds 50%. However, the use of these materials at higher operating temperatures is limited by their melting point. It has been shown that jet turbine components made of nickel-based alloys require constant cooling due to their relatively low melting point (~1400 °C), which reduces the efficiency and creates a gap between the performance of promising and currently existing engines.[5] Therefore, it is necessary to develop new materials capable of operating at higher temperatures than heat-resistant nickel alloys.

Cobalt-based alloys in the deformed and cast states are widely used to manufacture various parts of gas turbine engines and gas turbines, such as blades and combustion chambers. Recently, cobalt-based alloys have also been used in additive manufacturing.[6] These alloys are designed to enhance heat resistance due to solid-solution and carbide hardening. Carbon in cobalt alloys in an amount of 0.25 to 1 wt% promotes the formation of carbides, which also ensures the hardening of the material. The carbide network formed during solidification of the alloy is quite stable and provides strength at high temperatures.

In alloys X-40 and MAR-M509, the presence of a carbide network improves mechanical properties in the medium temperature range, but worsens creep resistance at high temperatures.[7] To provide resistance to oxidation and hot corrosion, cobalt-based alloys are alloyed with chromium, which provides resistance to sulfide-oxide corrosion, is a carbide-forming agent (M_7C_3, $M_{23}C_6$) and participates in the formation of the matrix intermetallic γ′-phase.

Nickel is introduced into cobalt alloys to stabilize the FCC structure.[8] Tungsten and molybdenum, like nickel, provide solid-solution hardening and are carbide formers (M_6C, MC). Tantalum and titanium also participate in solid-solution hardening and form MC carbides. Aluminum, yttrium and lanthanum are added to cobalt alloys to increase oxidation resistance. Zirconium and boron strengthen grain boundaries due to the formation of fine particles of carbides and borides, and carbon is involved in the formation of MC, M_6C, $M_{23}C_6$ and M_7C_3 carbides.[9,10] In recent years, refractory elements such as Re, Ta, W and Mo have been added to cobalt alloys to improve the high-temperature properties, which leads to an increase in heat resistance, creep resistance, improved anticorrosive properties of cobalt alloys and their resistance to oxidation.[11]

It should be noted that carbide-hardened cobalt-based heat-resistant alloys have a higher melting point and better corrosion resistance than nickel-based heat-resistant alloys, but are characterized by lower strength at high temperatures. The determining factor in the long-term strength of nickel and cobalt alloys is structural stability. Structural changes are caused by aging processes and are reduced due to the separation of carbides, the transformation of the γ′-phase or the formation of other intermetallic phases.

Iron–nickel alloys, which have superior properties, good machinability and lower cost than nickel-based alloys, are suitable for use at temperatures up to 680 °C.

Continuous advancements in materials technology contribute to the improvement of thermal resistance and overall performance of components made of ultra-high-strength alloys. One of the key challenges in developing next-generation superalloys is to improve their reliability and cost-effectiveness by reducing the content of expensive alloying elements. In addition, superalloys should contain a minimum amount of harmful impurities such as S, P, Pb, Bi and Te. Despite the existence of various heat-resistant alloys, the need to develop new materials capable of withstanding high mechanical loads at temperatures above 1000 K remains a pressing issue.

A novel class of materials that has recently attracted significant research interest is high-entropy alloys (HEAs). The primary distinguishing feature of HEAs is the formation of a single-phase, thermally stable solid solution with a body-centered cubic (BCC), face-centered cubic (FCC) or hexagonal close-packed (HCP) crystal structure. The development of an alloy or a series of new HEAs with properties surpassing those of existing nickel-based superalloys is unattainable without fundamental research into refractory metal-based alloys. A major obstacle to the widespread application of refractory metal-based HEAs as heat-resistant materials is the limited understanding of the mechanisms governing the formation of multicomponent solid solutions without long-range order and with pronounced lattice distortions, which are essential for

ensuring high mechanical performance even under extreme high-temperature operating conditions. Consequently, this issue is of both fundamental and applied significance.

Synthesis of refractory high-entropy alloys and investigation of their properties

A number of experimental and theoretical studies have been devoted to the analysis of the synthesis and properties of HEAs. Among them, several publications contain comprehensive reviews on the issues of manufacturing, characterization, structure and properties of multicomponent alloys.[12–34] It is worth noting that the vast majority of HEA research focuses on identifying new systems and compositions that form a single-phase solid solution. Most investigations are directed toward studying their structure, physical and mechanical properties, as well as the mechanisms of phase formation and the criteria for stabilizing a single phase in these multicomponent materials.

The selection of chemical elements comprising HEAs is determined by many factors, the most critical of which are related to the operating conditions of the material.[35]

A bulk of research has investigated HEAs based on refractory elements such as Hf, Ta, Mo, Nb, V, W, Cr, Zr and Ti.[36–41] The inclusion of refractory elements increases the melting temperature T_m of the alloy, making such alloys promising for high-temperature applications. In addition to refractory metals, heat-resistant HEAs may also contain components with relatively low melting points, provided that the alloy maintains high thermal stability. To enhance oxidation resistance, other alloying elements such as Al, Cr, Ti and Si are often added, or protective corrosion-resistant coatings are applied to the HEA surface.

The synthesis of HEAs, which form multicomponent solid solutions lacking long-range order and exhibiting significant lattice distortions, presents a complex task. Depending on the alloy composition and the desired properties, various fabrication methods are employed: mechanical alloying, which involves dynamic deformation of elemental powder blends in high-energy ball mills using different power densities and milling times; spark plasma sintering (SPS); the Bridgman solidification method, which involves heating raw materials above their melting points and then slowly cooling them in a specialized container; vacuum arc melting, in which the metal is melted using a transversely compressed electric arc as a heat source; additive manufacturing technique, a layer-by-layer fabrication approach utilizing metal powders based on a computer-generated 3D model.

The results of HEA synthesis carried out in recent years using these methods have been summarized in several review articles.[42,43]

Trofimenko *et al.*[44] explored the feasibility of synthesizing the VNbMoTaW HEA by hybrid spark plasma sintering from an equiatomic mixture of elemental powders (20 at% of each element) prepared by dry mixing. Compaction was performed at sintering temperatures of 1700, 1750 and 2000 °C. The findings indicate that increasing the sintering temperature from 1700 to 1750 °C leads to a wider diffusion zone, resulting in the formation of a quinary solid solution with a composition close to the equiatomic proportions defined during mixing. It was also established that while changing the temperature affects the diffusion processes, it does not eliminate the structural inhomogeneity, which is confirmed by microstructural analysis.

In another study,[45] a new method was proposed to synthesize the refractory AlTiZrVNb HEA *via* aluminothermic co-reduction of metals from their oxides. V and Nb were reduced and incorporated into the metallic phase to a degree of ~90%, while Ti and Zr showed lower reduction efficiencies (76 and 50%, respectively). The resulting alloy was multiphase, consisting of C14 Laves phases, Zr_5Al_3 type phases and an ordered B2 phase matrix. The microhardness of the alloy was 6.37 GPa, which is consistent with the values reported for refractory HEAs (RHEAs). The structure of the synthesized alloy was homogeneous throughout the bulk, exhibiting a coarse-grained morphology with some pores partially filled with non-metallic aluminum oxide inclusions.

In a recent work,[46] the researchers focused on the SPS of tungsten-containing HEA powders (WMoTaNb) and the investigation of the mechanical properties of the resulting samples. The synthesis was performed using the magnesiothermic reduction method, in which a mixture of metal oxides (WO_3, MoO_3, *etc.*) was reduced using magnesium. A specialized reactor was designed for this process, and various experimental conditions were tested, including the addition of retarders. The resulting powders were then consolidated using the SPS technology, which helps to retain the original microstructure of the powder. The sintering conditions were optimized to simultaneously control the chemical composition, grain growth and densification stages.

The development of RHEAs has led to the emergence of alloys with mechanical properties superior to those of conventional structural alloys, for example, with yield strengths exceeding 1000 MPa at temperatures below 600 °C.[15,43] However, similar to nickel-based superalloys, these new heat-resistant alloys are susceptible to degradation at elevated temperatures, limiting their effectiveness above 800 °C.

Exploration of the central regions of the phase space, limited by refractory elements (Nb, Ta, Zr, Hf, Mo and W), has resulted in the development of RHEAs capable of maintaining acceptable mechanical strength at temperatures up to 1600 °C.[43,47]

A comparative analysis of the physical and mechanical properties of RHEAs at ultra-high temperatures was conducted[48] with an emphasis on their behavior during hot deformation. The paper presents information on recent advances in the study of these alloy systems and discusses potential future research into RHEAs at extreme temperatures. The term ‘ultra-high temperature’ refers to temperatures at which the difficulties in technological testing become more pronounced. For modern nickel-based superalloys, this threshold does not exceed 1100 °C.[4]

Senkov *et al.*[49] investigated the properties of two heat-resistant HEAs, $Nb_{25}Mo_{25}Ta_{25}W_{25}$ and $V_{20}Nb_{20}Mo_{20}Ta_{20}W_{20}$, synthesized by vacuum arc melting. Both alloys had a single-phase BCC structure, which remained stable after thermal exposure up to 1400 °C. The Vickers hardness values of the alloys were determined to be 4.46 and 5.42 GPa, respectively, while their densities were measured to be 13.75 and 12.36 g cm^{-3}. The compressive properties were evaluated over the range from room temperature to 1600 °C. At room temperature, both alloys demonstrated high yield strengths (1058 and 1246 MPa, respectively) but limited ductility, with approximately 2 and 1% plastic strains for the quaternary and quinary alloys, respectively. In the temperature range of 600–1600 °C, both alloys maintained high yield strength and moderate ductility, although the $V_{20}Nb_{20}Mo_{20}Ta_{20}W_{20}$ alloy exhibited lower fracture strain. The results showed that the synthesized heat-resistant HEAs exhibited superior physical and mechanical properties compared to commercial alloys such as Inconel 718 and Haynes 230. Specifically, the yield strength values of the RHEAs were significantly higher than those of Haynes 230 over the entire temperature range studied and exceeded those of Inconel 718 at temperatures above 800 °C. According to the authors, the resistance of RHEAs to high-temperature softening compared to nickel-based superalloys is attributed to the slow diffusion of elements within the HEA matrix at temperatures up to 1600 °C,

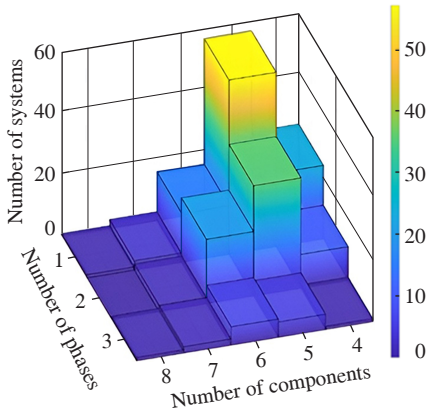

Figure 1 Diagram of the relationship between the number of components, the number of phases and the number of RHEAs. Reproduced from ref. 42 with permission. Copyright 2022 Uspekhi Khimii, ZIOC RAS, Russian Academy of Sciences and IOP Publishing Limited.

which is directly related to the high melting temperatures of the elements that comprise them.

Figure 1 presents a three-dimensional diagram comparing the number of refractory complex concentrated alloys with the number of phases and components they contain. The diagram is constructed based on the data from the sources cited above and our recent review.[42] It can be seen from this diagram that increasing the number of components and, consequently, increasing the ideal solid solution mixing entropy corresponding to that number does not always lead to the formation of a single-phase system. For example, the diagram shows that for senary alloys the number of two-phase systems exceeds the number of single-phase systems.

In the cited work,[50] the researchers present the results of an investigation into the refractory alloy $Ta_{20}Nb_{20}Hf_{20}Zr_{20}Ti_{20}$ synthesized by vacuum arc melting followed by hot isostatic pressing (HIP) at T = 1473 K and P = 207 MPa for 3 h. Figure 2 displays the results of X-ray diffraction analysis, demonstrating that the alloy has a single-phase BCC structure with a lattice constant of 340.4 pm both in the as-cast state and after HIP treatment. A minor peak at 2θ = 24.9° indicates the presence of a small fraction of a secondary phase, probably hexagonal.

The density and Vickers microhardness of the alloy after strengthening are 9.94 g cm^{-3} and 3826 MPa, respectively. The alloy exhibits significant strengthening, uniform deformation, high compressive yield strength of 929 MPa and ductility exceeding 50%.

The study of the refractory equiatomic HEA MoNbHfZrTi revealed that it is a disordered BCC solid solution in both the as-cast and homogenized states.[51] It was found that no phase transition occurs below 1743 K. At room temperature, the

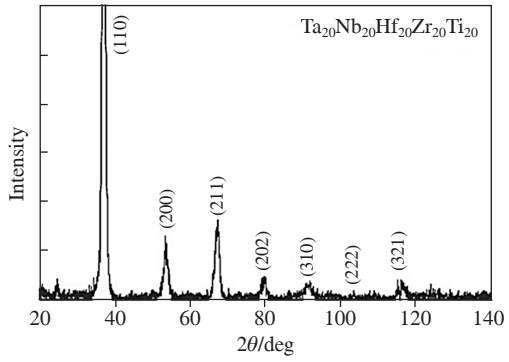

Figure 2 X-ray diffraction pattern of the TaNbHfZrTi alloy. Indexed peaks correspond to the BCC crystal lattice with a lattice constant of 340.4 pm. Reproduced from ref. 50 with permission. Copyright 2011 Elsevier.

compressive yield strengths of the alloy in the as-cast and homogenized states reach approximately 1719 and 1575 MPa, respectively, with a brittle quasi-cleavage fracture mechanism. At elevated temperatures, the compressive yield strength gradually decreases: 825 MPa at 1073 K, 728 MPa at 1173 K, 635 MPa at 1273 K, 397 MPa at 1373 K and 187 MPa at 1473 K. Additionally, a small amount of fine grains form along the grain boundaries due to partial dynamic recrystallization.

In the work by Ma *et al.*,[52] a novel refractory equiatomic HEA WTaHfTiZr was proposed as a potential material for next-generation thermonuclear reactors. The constituent elements were selected based on their low activation, high melting points and excellent thermal stability. The alloys were prepared using arc melting. The as-cast alloy was shown to exhibit a dendritic microstructure with two disordered BCC phases. This two-phase BCC structure is attributed to the preferential formation of W- and Ta-rich crystals during solidification, which have significantly higher melting points. The dendritic BCC phase is enriched in high-melting point elements (W and Ta), while the interdendritic BCC phase is enriched in lower-melting point elements (Hf, Ti and Zr). At room temperature, the alloy exhibits a high compressive yield strength of 1900 MPa and a fracture strain of 8.1%. The compressive yield strength at elevated temperatures reaches 612 MPa at 700 °C and 203 MPa at 1000 °C.

Senkov *et al.*[53] reported on the mechanical properties of four heat-resistant alloys, NbTiVZr, $NbTiV_2Zr$, CrNbTiZr and CrNbTiVZr, at room and elevated temperatures. These alloys were synthesized using vacuum arc melting followed by HIP and homogenization. The primary phases in these alloys were identified as disordered BCC solid solution phases. The alloys containing Cr additionally exhibited ordered Laves phases. The densities of the alloys were 6.52, 6.34, 6.67 and 6.57 g cm^{-3}, respectively. NbTiVZr and $NbTiV_2Zr$ alloys demonstrated good compressive ductility at all temperatures studied, whereas the Cr-containing alloys exhibited a brittle-to-ductile transition in the temperature range of 298–873 K. Notably, NbTiVZr and $NbTiV_2Zr$ showed pronounced work hardening at room temperature. These alloys had initial yield strengths of 1105 and 918 MPa, respectively, with compressive strengths exceeding 2000 MPa after 40% strain. CrNbTiZr and CrNbTiVZr alloys displayed high yield strengths (1260 and 1298 MPa, respectively), but limited ductility (6 and 3% compressive strain) at room temperature. At temperatures above 873 K, these alloys showed softening and steady-state flow during compression, withstanding 50% strain without failure, with the yield strength gradually decreasing as the temperature increased. At 1273 K, the yield strengths of NbTiVZr, $NbTiV_2Zr$, CrNbTiZr and CrNbTiVZr were 58, 72, 115 and 259 MPa, respectively.

Promising heat-resistant HEAs $Nb_{30}Mo_{30}Co_{20}Hf_{20}$, $Nb_{30}Mo_{30}Co_{20}Zr_{20}$ and $Nb_{30}Mo_{30}Co_{20}Ti_{20}$ have been developed in the Laboratory of Bulk Nanostructured Materials at Belgorod State University (Russia).[54] These alloys consist of an B2 intermetallic matrix, disordered BCC phase particles and a small volume fraction of additional BCC phases (in $Nb_{30}Mo_{30}Co_{20}Hf_{20}$ and $Nb_{30}Mo_{30}Co_{20}Zr_{20}$) or FCC phases (in $Nb_{30}Mo_{30}Co_{20}Ti_{20}$). Uniaxial compression tests have revealed that $Nb_{30}Mo_{30}Co_{20}Ti_{20}$ exhibits a higher yield strength in the temperature range of 22–1000 °C compared to $Nb_{30}Mo_{30}Co_{20}Hf_{20}$ and $Nb_{30}Mo_{30}Co_{20}Zr_{20}$. While $Nb_{30}Mo_{30}Co_{20}Zr_{20}$ remained unfractured at 22–800 °C under 50% strain, $Nb_{30}Mo_{30}Co_{20}Ti_{20}$ was found to be brittle. All developed alloys demonstrated a high degree of work hardening in the range of 22–800 °C and exhibited specific strengths comparable to commercial nickel- and cobalt-based superalloys.

One of the major obstacles to the widespread adoption of RHEAs is their low resistance to oxidation at high temperatures.[55] To fabricate new heat-resistant RHEA compositions new elements that enhance oxidation resistance, such as Al, Cr, Ti and Si, have been successfully alloyed.[56–58]

Since changes in surface composition due to oxidation play a crucial role in maintaining material properties, a detailed thermodynamic description of the oxygen adsorption mechanism on such complex surfaces is needed. The interaction of oxygen with the surface of the refractory alloy MoWTaTiZr was investigated,[59] providing an explanation based on first-principles and atomistic thermodynamic models. The RHEA surface exhibits high reactivity with oxygen, forming a monolayer in the temperature range of 300–1500 K. The preferential adsorption of oxygen at specific surface sites is attributed to the electron configuration of the bonding orbitals of the constituent surface atoms. As oxygen continues to accumulate, its atoms diffuse into the bulk regions of the alloy. Temperature and oxygen pressure variations indicate that oxygen removal from the alloy surface is challenging, even at extremely low oxygen pressures of 10^{-9} bar at 2000 K.

Another key property of RHEAs is their density, which determines the magnitude of inertia stresses that can develop within components, which is especially critical for rotating machinery. The addition of lightweight metals (Al, Ti or V) has led to the development of RHEAs with a density of only 5.45 g cm^{-3}.[15] Unsurprisingly, there is a trade-off between low weight and high-temperature strength: denser alloys generally exhibit greater strength at elevated temperatures. For instance, the MoNbTaW alloy has a yield strength of 400 MPa at 1600 °C, making it one of the strongest RHEAs at extreme temperatures.

In domestic and foreign literature, works have been published on the development of HEA coatings, which can serve as functional layers in the manufacture or restoration of machine parts operating under extreme loads. The base parts themselves can be made of traditional, relatively inexpensive metals and alloys, making the application of HEA coatings technically and economically justified.[37,38,60–67]

A brief review of foreign and domestic scientific publications on the study of the structure, phase composition and properties of films and coatings of five-component HEAs on various substrates and modification of HEA surfaces by various types of processing, including magnetron sputtering, thermal spraying, laser spraying and electrodeposition, is presented by Gromov *et al.*[63] It is shown that improvement of tribological and strength properties, as well as corrosion resistance of film coatings, is observed in a wide range of temperatures.

The results of the study of RHEAs HfNbTaZr and MoNbTaVW for high temperature aerospace and power engineering applications are presented by Dixit *et al.*[64] Atmospheric plasma spraying and high velocity oxygen fuel processes were used to deposit RHEA coatings on SS 321 and Inconel 718 since these alloys are widely used in industry. HfNbTaZr was selected because it is suitable for harsh environments without nuclear reactor radiation, while MoNbTaVW is suitable for harsh environments including radiation. These coatings are shown to have excellent adhesion properties and high strength, as well as reasonable homogeneity and deposition characteristics. Thus, RHEA coatings may be suitable for use in harsh environments due to their abrasion resistance, increased hardness and high-entropy composition of high-temperature refractory elements. Experimental data[64] also indicate great potential for RHEA coatings to reduce erosion and provide high-temperature structural integrity in sCO_2 Brayton Cycles, turbomachinery (*e.g.*, diffusers and turbine blades), aerospace components (components based on Inconel 718) and advanced nuclear reactors.

At the Institute of High Current Electronics of the Siberian Branch of the Russian Academy of Sciences, multilayer metal–ceramic coatings based on the refractory TiNbZrTaHf HEA were formed by the plasma-assisted vacuum-arc deposition method.[65] It was shown that the coatings are a nanomaterial with a nanocrystal size of 2.5–4 nm. The metal layer has a BCC crystal lattice (a = 3.3396 Å). Using X-ray phase analysis methods, it was determined that the ceramic layer is two-phase, (TiNbZrTaHf)N + Ta_4N. The nitride (TiNbZrTaHf)N has an FCC crystal lattice with the parameter a = 4.4465 Å (D = 22 nm, $\Delta d/d = 7 \times 10^{-3}$). Nitride Ta_4N has a tetragonal crystal lattice with the parameters a = 6.8272 and c = 4.1697 Å (D = 10 nm, $\Delta d/d = 7 \times 10^{-3}$). The formation of transition layers between the substrate and the metal layer, as well as between the metal and ceramic layers, was revealed. The coating hardness was 36.7 GPa, and Young's modulus 323 GPa. The authors of the work under consideration note the prospects for using HEA-based coatings as protective coatings for tools and parts of a wide range of applications.

Solid-state cold spray deposition was used for the first time to create the HEA FeCoNiCrMn coating.[66] This method enabled the production of HEA coatings with a high growth rate and low porosity [Figure 3(*a*)]. Importantly, the phase structure of the HEA was completely preserved in the coating, without any phase transformations [Figure 3(*b*)]. The grains in the HEA coating were significantly finer than those in the original HEA powder, which was associated with dynamic recrystallization in the highly deformed interparticle region [Figure 3(*c*)]. Due to the increased density of dislocations and grain boundaries, the HEA coatings obtained by cold spraying had a significantly higher hardness than the original powdered material, which led to enhanced wear resistance.

Refractory NbTaMoW thin films with near-equiatomic composition were deposited by ion beam sputtering at room temperature.[67] The study demonstrated uniform distribution of

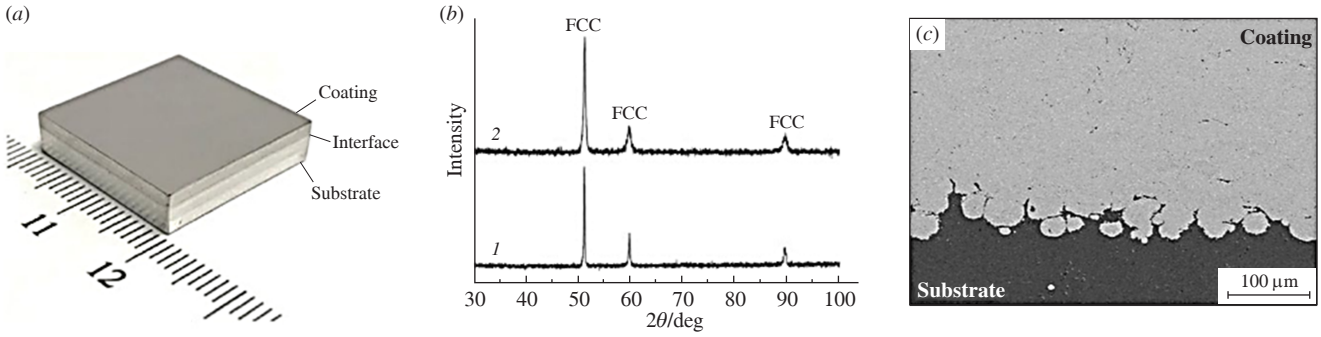

Figure 3 Characteristics of the HEA FeCoNiCrMn coating obtained by solid-state cold spraying: (*a*) photograph of the HEA coating after post-spray processing, (*b*) X-ray diffraction patterns of (*1*) the HEA powder and (*2*) the HEA coating, and (*c*) SEM image of the cross-section of the HEA coating. Reproduced from ref. 66 with permission. Copyright 2019 Elsevier.

all elements and consistent BCC crystal structure in the samples. Transmission electron microscopy images revealed large columnar grains and the presence of Ar bubbles with an average diameter of 1.3 ± 0.4 nm. The article discusses growth mechanisms of the films, based on high-entropy film characteristics, classical nucleation and growth theory and the Movchan–Demchishin–Thornton structure zone model. Nanoindentation measurements showed that the films had a hardness of 22.8 ± 0.7 GPa. Additionally, nanodispersion analysis indicated that the exceptional hardness is also associated with high resistance to cracking and delamination, suggesting high impact strength and fracture toughness. The obtained results indicate that the combination of refractory metals with the properties inherent in HEAs leads to the creation of reliable NbTaMoW coatings for applications in extreme conditions.

There is no doubt that the HEAs range will continue to expand.

In addition to the development of new materials and the study of their properties, the most important area of research is the study of the behavior of HEAs under extreme conditions, including aggressive chemical environments, high and cryogenic temperatures, extreme pressures, *etc*.

Computer modeling

However, it should be noted that the experimental study of the properties of metals and alloys at high temperatures is associated with a number of challenges. In particular, it is difficult to ensure adiabatic conditions for the sample and accurately take into account the heat exchange between the sample and the environment. In addition, at high temperatures, intense oxidation strongly affects the experimental data.

Therefore, it is currently believed that the development and investigation of complex multifunctional structures are impossible without preliminary thermodynamic analysis. The advantages of chemical thermodynamics for solving these problems are greatly enhanced by the widespread use of computer technologies.

Thermodynamic studies are necessary to determine appropriate technological regimes of material production and related design features of equipment. They also have the potential to predict various properties of materials obtained under real conditions, thus being the basis for controlled synthesis of various materials, including HEAs.[39,68–72]

The number of publications on atomistic modeling of HEA properties has increased dramatically over the past decade. According to the Scopus database, the number of articles on the topic ‘high entropy alloys’ AND ‘molecular dynamics’ increased from 4 in 2014 to 171 per year in 2023. However, these numbers remain modest compared to the total number of HEA-related publications, which amounted to 3010 in 2023. This is explained by the inherent difficulties in atomistic modeling of HEAs. The large compositional space of HEAs complicates their investigation using *ab initio* methods such as density functional theory. At the same time, classical molecular dynamics (as well as the classical Monte Carlo method) requires highly accurate knowledge of interatomic interactions, which are failed to be reproduced using traditional interaction potentials for multicomponent systems.

A possible solution to this problem lies in the rapidly developing field of machine learning-based potentials. Although such potentials provide accuracy comparable to *ab initio* calculations and significantly outperform them in computational efficiency, it is still relatively low compared to calculations using traditional interatomic potentials of classical molecular dynamics. Therefore, for calculating mechanical strength properties, which require simulation cells containing millions of atoms on relatively long time scales, researchers prefer to use high-performance (M)EAM models.[72,73] Meanwhile, machine learning-based potentials in HEA research are primarily used for modeling melt properties.[74,75]

However, an exception to the above approach can be found.[76] Using the Moment Tensor Potential parameterized from *ab initio* data, a machine learning model was developed by A. V. Shapeev at Skolkovo.[77] The study employed classical molecular dynamics to investigate screw and edge dislocations in the MoNbTaW system containing 573 672 atoms. But even such a seemingly large number of atoms is not enough for direct modeling of plastic deformation, which is necessary to evaluate the mechanical properties of the crystal. For instance, in the work of Zepeda-Ruiz *et al.*,[78] where plastic deformation of a tantalum single crystal was modeled, simulation cells containing tens and even hundreds of millions of atoms were used. Despite this, the authors were not entirely sure that they managed to completely eliminate the so-called finite size effects. Thus, direct atomistic modeling of plastic deformation in crystals is extremely challenging due to its high computational cost. Nevertheless, this does not mean that atomistic modeling methods cannot be used to predict the high-temperature properties of HEAs.

The high-temperature strength of HEAs is influenced by many factors, which can be estimated using atomistic modeling. Of primary importance are dislocations and their interactions with each other and with other defects in the material, such as point defects (vacancies, substitutional atoms and interstitial atoms), two-dimensional defects (grain boundaries, twinning planes and stacking faults) and second-phase inclusions. Additionally, the resistance of HEAs to high-temperature oxidation is a critical factor. This resistance can be enhanced, for example, by applying protective coatings to the metal, which in turn requires compatibility of the elastic and thermophysical properties of both the metal and the protective coating. Thus, a comprehensive and thorough assessment of the high-temperature strength of HEAs using atomistic modeling can be achieved by calculating the properties of point, line, planar and three-dimensional defects; by investigating the interactions of HEAs with oxygen and protective coatings; by evaluating the thermophysical and elastic properties of HEAs and coatings; and also by analyzing the phase composition. Below are some of the most recent studies published in the literature that have used atomistic modeling to explore these aspects.

Molecular dynamics was used to investigate the effect of vacancy concentration on the mechanical properties of HEA FeNiCoCrCu.[79] Uniaxial tension simulations were conducted on a system consisting of 108 000 atoms with varying vacancy concentrations. The study revealed the reasons for the reduction in the mechanical strength of FeNiCoCrCu as the vacancy concentration increased. This work was carried out using the EAM potential.

The $FeNiCoCrCu_x$ nanopolycrystal was analyzed using a combined molecular dynamics and Monte Carlo approach.[80] The research revealed patterns of atoms segregation at grain boundaries, indicating that copper preferentially accumulates at these interfaces. It was observed that increasing the copper concentration in the HEA initially enhances its strength. However, further increasing the copper content deteriorates the mechanical properties of $FeNiCoCrCu_x$, since excess copper atoms at the grain boundaries lead to crack formation. This study was conducted using the EAM potential.

The formation of twins was considered in molecular dynamics simulations of the interaction between a Cantor alloy (CoCrFeMnNi) and a nanoindenter for both single crystal and twinned bicrystal cases.[81] The results demonstrated that the twinning plane serves as a glide path for dislocations generated

under load. The study was conducted using a simulation cell containing more than a million atoms and the EAM potential.

Phase stability data were obtained using *ab initio* atomistic calculations in a study of the electronic, magnetic and vibrational contributions to the free energy of the Cantor alloy (CoCrFeMnNi).[82] These calculations determined the relative thermodynamic stability of its constituent BCC, FCC and HCP phases.

The interaction of HEAs with oxygen was studied using a hybrid Molecular Dynamics–Monte Carlo (first principles calculation) method by simulating the interaction of HEA FeCoNiCuPt nanoparticles with oxygen molecules.[83]

Thermophysical properties of HEAs have also been studied using classical molecular dynamics. For example, for HEA $Al_{0.3}$CoCrFeNi, such thermophysical properties as lattice thermal conductivity, heat capacity and thermal expansion coefficient were calculated using this method.[84] This work was conducted using the EAM potential. It is crucial to note that in metals, the electronic subsystem makes a significant contribution to the thermal conductivity. To account for this, a two-temperature model (TTM) is commonly used.[85] In a recently published study,[86] the researchers successfully combined the temperature-dependent DeePMD machine learning potential[87] with the TTM approach for pure tungsten.

At this stage, research into the atomistic modeling of HEA properties, particularly those related to high-temperature strength, remains unsystematic. Only specific properties of selected alloys representing a small fraction of all possible HEA compositions have been studied. This is due to the lack of interatomic potentials that are simultaneously reliable, universal and computationally efficient, as well as the vast number of possible HEA compositions. Ongoing efforts to develop universal interatomic potentials[88–90] could lead to the creation of the required models. However, it is currently unclear how widely these potentials can be applied to study the high-temperature strength of HEAs, as they may still lack accuracy and computational efficiency.

Conclusion

This literature review demonstrates the promising potential of HEAs as heat-resistant materials that can compete with nickel- and cobalt-based superalloys. However, RHEAs also exhibit notable drawbacks, primarily high density and brittleness. Existing low-density heat-resistant HEAs generally lack high-temperature strength, with the exception of NbMoCrTiAl, which exhibited a yield strength of 600 MPa at 1000 °C. However, this alloy is extremely brittle at room temperature.

In Russia, active research in this field is conducted by scientists from Belgorod State University (Belgorod), the N. A. Vatolin Institute of Metallurgy of the Ural Branch of the Russian Academy of Sciences (Ekaterinburg), the A. G. Merzhanov Institute of Structural Macrokinetics and Materials Science of the Russian Academy of Sciences (Chernogolovka, Moscow Region), the Ural Federal University (Ekaterinburg), the South Ural State University (Chelyabinsk) and the All-Russian Scientific Research Institute of Aviation Materials (Moscow).

Internationally, active research is being conducted by scientists from China (Tsinghua University, Beijing; Sun Yat-Sen University, Guangzhou; Chinese Academy of Sciences; Huazhong University of Science and Technology, Wuhan; China Iron and Steel Research Institute Group, Beijing, among others), France (Université de Bourgogne Franche-Comté, Dijon; Université Paris; Université Paris Est Creteil), United Kingdom (Institute for Materials Research, University of Huddersfield; Department of Materials, University of Oxford), Austria (Department of Materials Physics, University of Leoben), Australia (University of New South Wales, Sydney) and United States (Air Force Research Laboratory, Materials and Manufacturing Directorate, Dayton; Department of Engineering Physics, University of Wisconsin-Madison). Additionally, Belarusian researchers continue to contribute to this field, now as part of the international research community.

Thus, the development of new RHEAs with superior strength characteristics compared to nickel-based superalloys remains a highly relevant scientific task.

This work was financially supported by the Russian Science Foundation (grant no. 25-43-00148).

References

1 N. R. Philips, M. Carl and N. J. Cunningham, *Metall. Mater. Trans. A*, 2020, **51**, 3299; https://doi.org/10.1007/s11661-020-05803-3.
2 E. Akca and A. Gürsel, *Periodicals of Engineering and Natural Sciences*, 2015, **3** (1), 15; https://web.archive.org/web/20231023142938/http://pen.ius.edu.ba/index.php/pen/article/view/43.
3 A. Kollová and K. Pauerová, *Manufacturing Technology*, 2022, **22**, 550; https://doi.org/10.21062/mft.2022.070.
4 J. Rame, S. Utada, L. M. Bortoluci Ormastroni, L. Mataveli-Suave, E. Menou, L. Després, P. Kontis and J. Cormier, in *Superalloys 2020: Proceedings of the 14th International Symposium on Superalloys*, eds. S. Tin, M. Hardy, J. Clews, J. Cormier, Q. Feng, J. Marcin, C. O'Brien and A. Suzuki, Springer, Cham, 2020, pp. 71–81; https://doi.org/10.1007/978-3-030-51834-9_7.
5 J. H. Perepezko, *Science*, 2009, **326**, 1068; https://doi.org/10.1126/science.1179327.
6 P. B. Mazalov, D. I. Suhov, E. A. Sulyanova and I. S. Mazalov, *Aviation Materials and Technologies*, 2021, no. 3, 3; https://doi.org/10.18577/2713-0193-2021-0-3-3-10.
7 Yu. G. Veksler, L. A. Mal'tseva and M. V. Pastukhov, *Russ. Metall.*, 2015, 244; https://doi.org/10.1134/S003602951503012X.
8 P. Zhou, X. Gao, D. Song, Y. Liu and J. Cheng, *Scanning*, 2021, 6678085; https://doi.org/10.1155/2021/6678085.
9 R. Liu, M. X. Yao and X. Wu, *J. Eng. Mater. Technol.*, 2004, **126**, 204; https://doi.org/10.1115/1.1651096.
10 M. A. L. Hernandez-Rodriguez, D. A. Laverde-Cataño, D. Lozano, G. Martinez-Cazares and Y. Bedolla-Gil, *Metals*, 2019, **9**, 307; https://doi.org/10.3390/met9030307.
11 X. Liu, D. Wu, J. Zhang, M. Yang, J. Zhu, L. Li, Y. Chen, S. Yang, J. Han, Y. Lu and C. Wang, *Metals*, 2018, **8**, 911; https://doi.org/10.3390/met8110911.
12 Y. Zhang, *High-Entropy Materials: A Brief Introduction*, Springer, Singapore, 2019; https://doi.org/10.1007/978-981-13-8526-1.
13 Y. Zhang, T. T. Zuo, Z. Tang, M. C. Gao, K. A. Dahmen, P. K. Liaw and Z. P. Lu, *Prog. Mater. Sci.*, 2014, **61**, 1; https://doi.org/10.1016/j.pmatsci.2013.10.001.
14 B. Cantor, *Entropy*, 2014, **16**, 4749; https://doi.org/10.3390/e16094749.
15 D. B. Miracle and O. N. Senkov, *Acta Mater.*, 2017, **122**, 448; https://doi.org/10.1016/j.actamat.2016.08.081.
16 *High-Entropy Alloys: Fundamentals and Applications*, eds. M. C. Gao, J.-W. Yeh, P. K. Liaw and Y. Zhang, Springer, Cham, 2016; https://doi.org/10.1007/978-3-319-27013-5.
17 W. Zhang, P. K. Liaw and Y. Zhang, *Sci. China Mater.*, 2018, **61**, 2; https://doi.org/10.1007/s40843-017-9195-8.
18 B. S. Murty, J. W. Yeh and S. Ranganathan, *High-Entropy Alloys*, Elsevier, Amsterdam, 2014; https://doi.org/10.1016/C2013-0-14235-3.
19 B. S. Murty, J. W. Yeh, S. Ranganathan and P. P. Bhattacharjee, *High-Entropy Alloys*, 2nd edn., Elsevier, Amsterdam, 2019; https://doi.org/10.1016/C2017-0-03317-7.
20 E. P. George, D. Raabe and R. O. Ritchie, *Nat. Rev. Mater.*, 2019, **4**, 515; https://doi.org/10.1038/s41578-019-0121-4.
21 A. D. Pogrebnjak, A. A. Bagdasaryan, I. V. Yakushchenko and V. M. Beresnev, *Russ. Chem. Rev.*, 2014, **83**, 1027; https://doi.org/10.1070/rcr4407.
22 Z. B. Bataeva, A. A. Ruktuev, I. V. Ivanov, A. B. Yurgin and I. A. Bataev, *Obrabotka Metallov*, 2021, **23** (2), 116 (in Russian); https://doi.org/10.17212/1994-6309-2021-23.2-116-146.
23 J.-W. Yeh, S.-K. Chen, S.-J. Lin, J.-Y. Gan, T.-S. Chin, T.-T. Shun, C.-H. Tsau and S.-Y. Chang, *Adv. Eng. Mater.*, 2004, **6**, 299; https://doi.org/10.1002/adem.200300567.

24 T. K. Chen, T. T. Shun, J. W. Yeh and M. S. Wong, *Surf. Coat. Technol.*, 2004, **188**–**189**, 193; https://doi.org/10.1016/j.surfcoat.2004.08.023.
25 M. Feuerbacher, T. Lienig and C. Thomas, *Scr. Mater.*, 2018, **152**, 40; https://doi.org/10.1016/j.scriptamat.2018.04.009.
26 A. S. Rogachev, *Phys. Met. Metallogr.*, 2020, **121**, 733; https://doi.org/10.1134/S0031918X20080098.
27 S. Uporov, V. Bykov, S. Pryanichnikov, A. Shubin and N. Uporova, *Intermetallics*, 2017, **83**, 1; https://doi.org/10.1016/j.intermet.2016.12.003.
28 O. S. Bamisaye, N. Maledi, J. Van der Merwe, D. E. P. Klenam, M. O. Bodunrin and A. D. Akinwekomi, *Manuf. Rev.*, 2023, **10**, 12; https://doi.org/10.1051/mfreview/2023008.
29 X. Ren, Y. Li, Y. Qi and B. Wang, *Materials*, 2022, **15**, 2931; https://doi.org/10.3390/ma15082931.
30 K. Cui and Y. Zhang, *Coatings*, 2023, **13**, 635; https://doi.org/10.3390/coatings13030635.
31 C. Zhang and Y. Yang, *MRS Bull.*, 2022, **47**, 158; https://doi.org/10.1557/s43577-022-00284-8.
32 M.-H. Tsai and J.-W. Yeh, *Mater. Res. Lett.*, 2014, **2**, 107; https://doi.org/10.1080/21663831.2014.912690.
33 K. A. Osintsev, V. E. Gromov, S. V. Konovalov, Yu. F. Ivanov and I. A. Panchenko, *Steel in Translation*, 2022, **52**, 167; https://doi.org/10.3103/S0967091222020176.
34 Y. Y. Kambarov, G. K. Uazyrkhanova, M. Rutkowska-Gorczyca and A. Y. Kussainov, *NNC RK Bulletin*, 2023, no. 1, 25; https://doi.org/10.52676/1729-7885-2023-1-25-39.
35 N. N. Trofimenko, I. Yu. Efimochkin and A. N. Bolshakova, *Aviation Materials and Technologies*, 2018, no. 2, 3; https://doi.org/10.18577/2071-9140-2018-0-2-3-8.
36 A. A. Rempel and B. R. Gelchinski, *Steel in Translation*, 2020, **50**, 243; https://doi.org/10.3103/S0967091220040075.
37 A. D. Pogrebnjak, V. M. Beresnev, A. V. Bondar', M. V. Kaverin and A. G. Ponomarev, *Russ. Phys. J.*, 2013, **56**, 532; https://doi.org/10.1007/s11182-013-0065-x.
38 A. D. Pogrebnjak, *J. Nanomater.*, 2013, 780125; https://doi.org/10.1155/2013/780125.
39 B. R. Gelchinski, I. A. Balyakin, N. I. Ilinykh and A. A. Rempel, *Phys. Mesomech.*, 2021, **24**, 701; https://doi.org/10.1134/S1029959921060084.
40 H. Qiu, X. Yan, S. Wu, W. Jiang, B. Zhu and S. Guo, *Coatings*, 2023, **13**, 1650; https://doi.org/10.3390/coatings13091650.
41 V. M. Yurov, S. A. Guchenko, V. I. Goncharenko and V. S. Oleshko, *J. Phys.: Conf. Ser.*, 2021, **2064**, 012080; https://doi.org/10.1088/1742-6596/2064/1/012080.
42 B. R. Gelchinski, I. A. Balyakin, A. A. Yuryev and A. A. Rempel, *Russ. Chem. Rev.*, 2022, **91**, RCR5023; https://doi.org/10.1070/RCR5023.
43 O. N. Senkov, D. B. Miracle, K. J. Chaput and J.-P. Couzinie, *J. Mater. Res.*, 2018, **33**, 3092; https://doi.org/10.1557/jmr.2018.153.
44 N. N. Trofimenko, I. Yu. Efimochkin, I. V. Osin and R. M. Dvoretskov, *Aviation Materials and Technologies*, 2019, no. 2, 12; https://doi.org/10.18577/2071-9140-2019-0-2-12-20.
45 E. M. Zhilina, A. S. Russkih, T. V. Osinkina, E. V. Ignatieva, S. A. Petrova, S. A. Krasikov, A. V. Dolmatov and A. A. Rempel, *Russ. Chem. Bull.*, 2023, **72**, 895; https://doi.org/10.1007/s11172-023-3852-7.
46 M. Moser, S. Dine, D. Vrel, L. Perrière, R. Pirès-Brazuna, H. Couque and F. Bernard, *Materials*, 2022, **15**, 5416; https://doi.org/10.3390/ma15155416.
47 O. N. Senkov, G. B. Wilks, D. B. Miracle, C. P. Chuang and P. K. Liaw, *Intermetallics*, 2010, **18**, 1758; https://doi.org/10.1016/j.intermet.2010.05.014.
48 K. C. Atli and I. Karaman, *Frontiers in Metals and Alloys*, 2023, **2**, 1135826; https://doi.org/10.3389/ftmal.2023.1135826.
49 O. N. Senkov, G. B. Wilks, J. M. Scott and D. B Miracle, *Intermetallics*, 2011, **19**, 698; https://doi.org/10.1016/j.intermet.2011.01.004.
50 O. N. Senkov, J. M. Scott, S. V. Senkova, D. B. Miracle and C. F. Woodward, *J. Alloys Compd.*, 2011, **509**, 6043; https://doi.org/10.1016/j.jallcom.2011.02.171.
51 N. N. Guo, L. Wang, L. S. Luo, X. Z. Li, Y. Q. Su, J. J. Guo and H. Z. Fu, *Mater. Des.*, 2015, **81**, 87; https://doi.org/10.1016/j.matdes.2015.05.019.
52 X. Ma, Y. Hu, K. Wang, H. Zhang, Z. Fan, J. Suo and X. Liu, *China Foundry*, 2022, **19**, 489; https://doi.org/10.1007/s41230-022-1230-z.
53 O. N. Senkov, S. V. Senkova, D. B. Miracle and C. Woodward, *Mater. Sci. Eng., A*, 2013, **565**, 51; https://doi.org/10.1016/j.msea.2012.12.018.
54 E. S. Panina, N. Yu. Yurchenko, A. A. Tozhibaev, M. V. Mishunin, S. V. Zherebtsov and N. D. Stepanov, *Phys. Mesomech.*, 2023, **26**, 666; https://doi.org/10.1134/S1029959923060061.
55 S. Veselkov, O. Samoilova, N. Shaburova and E. Trofimov, *Materials*, 2021, **14**, 2595; https://doi.org/10.3390/ma14102595.
56 B. Gorr, S. Schellert, F. Müller, H.-J. Christ, A. Kauffmann and M. Heilmaier, *Adv. Eng. Mater.*, 2021, **23**, 2001047; https://doi.org/10.1002/adem.202001047.
57 S. Sheikh, L. Gan, T.-K. Tsao, H. Murakami, S. Shafeie and S. Guo, *Intermetallics*, 2018, **103**, 40; https://doi.org/10.1016/j.intermet.2018.10.004.
58 F. Müller, B. Gorr, H.-J. Christ, J. Müller, B. Butz, H. Chen, A. Kauffmann and M. Heilmaier, *Corros. Sci.*, 2019, **159**, 108161; https://doi.org/10.1016/j.corsci.2019.108161.
59 E. Osei-Agyemang and G. Balasubramanian, *npj Mater. Degrad.*, 2019, **3**, 20; https://doi.org/10.1038/s41529-019-0082-5.
60 X. Zhang, N. Zhang, B. Xing and S. Yin, *J. Therm. Spray Technol.*, 2022, **31**, 1386; https://doi.org/10.1007/s11666-022-01352-w.
61 S. K. Padamata, A. Yasinskiy, V. Yanov and G. Saevarsdottir, *Metals*, 2022, **12**, 319; https://doi.org/10.3390/met12020319.
62 C.-T. Lee, W.-H. Cho, M.-H. Shiao, C.-N. Hsiao, K.-S. Tang and C.-C. Jaing, *Procedia Eng.*, 2012, **36**, 316; https://doi.org/10.1016/j.proeng.2012.03.046.
63 V. E. Gromov, S. V. Konovalov, O. A. Peregudov, M. O. Efimov and Yu. A. Shlyarova, *Steel in Translation*, 2022, **52**, 899; https://doi.org/10.3103/S0967091222100047.
64 S. Dixit, S. Rodriguez, M. R. Jones, P. Buzby, R. Dixit, N. Argibay, F. W. DelRio, H. H. Lim and D. Fleming, *J. Therm. Spray Technol.*, 2022, **31**, 1021; https://doi.org/10.1007/s11666-022-01324-0.
65 Y. F. Ivanov, Y. Kh. Akhmadeev, O. V. Krysina, N. N. Koval, V. V. Shugurov, E. A. Petrikova, N. A. Prokopenko and O. S. Tolkachev, *Coatings*, 2023, **13**, 1381; https://doi.org/10.3390/coatings13081381.
66 S. Yin, W. Li, B. Song, X. Yan, M. Kuang, Y. Xu, K. Wen and R. Lupoi, *J. Mater. Sci. Technol.*, 2019, **35**, 1003; https://doi.org/10.1016/j.jmst.2018.12.015.
67 M. A. Tunes and V. M. Vishnyakov, *Mater. Des.*, 2019, **170**, 107692; https://doi.org/10.1016/j.matdes.2019.107692.
68 Y. Zhou, P. Srinivasan, F. Körmann, B. Grabowski, R. Smith, P. Goddard and A. I. Duff, *Phys. Rev. B*, 2022, **105**, 214302; https://doi.org/10.1103/PhysRevB.105.214302.
69 M. Mukarram, M. A. Munir, M. Mujahid and K. Yaqoob, *Metals*, 2021, **11**, 1484; https://doi.org/10.3390/met11091484.
70 K. S. N. Satish Idury, B. S. Murty and J. Bhatt, *Intermetallics*, 2015, **65**, 42; https://doi.org/10.1016/j.intermet.2015.04.007.
71 Yu. A. Mityushova, A. F. Gibadullina, E. M. Zhilina, A. S. Russkikh and S. A. Krasikov, *Russ. Metall.*, 2021, 187; https://doi.org/10.1134/S0036029521020166.
72 J. Li, Q. Fang, B. Liu, Y. Liu and Y. Liu, *RSC Adv.*, 2016, **6**, 76409; https://doi.org/10.1039/C6RA16503F.
73 K.-T. Chen, T.-J. Wei, G.-C. Li, M.-Y. Chen, Y.-S. Chen, S.-W. Chang, H.-W. Yen and C.-S. Chen, *Mater. Chem. Phys.*, 2021, **271**, 124912; https://doi.org/10.1016/j.matchemphys.2021.124912.
74 I. A. Balyakin, A. A. Yuryev, B. R. Gelchinski and A. A. Rempel, *J. Phys.: Condens. Matter*, 2020, **32**, 214006; https://doi.org/10.1088/1361-648X/ab6f87.
75 S. A. Uporov, E. V. Sterkhov, I. A. Balyakin, V. A. Bykov, I. S. Sipatov and A. A. Rempel, *Intermetallics*, 2024, **165**, 108121; https://doi.org/10.1016/j.intermet.2023.108121.
76 S. Yin, Y. Zuo, A. Abu-Odeh, H. Zheng, X.-G. Li, J. Ding, S. P. Ong, M. Asta and R. O. Ritchie, *Nat. Commun.*, 2021, **12**, 4873; https://doi.org/10.1038/s41467-021-25134-0.
77 A. V. Shapeev, *Multiscale Model. Simul.*, 2016, **14**, 1153; https://doi.org/10.1137/15M1054183.
78 L. A. Zepeda-Ruiz, A. Stukowski, T. Oppelstrup and V. V. Bulatov, *Nature*, 2017, **550**, 492; https://doi.org/10.1038/nature23472.
79 J. Peng, B. Xie, X. Zeng, Q. Fang, B. Liu, P. K. Liaw and J. Li, *Int. J. Mech. Sci.*, 2022, **218**, 107065; https://doi.org/10.1016/j.ijmecsci.2022.107065.
80 T. He, Y. Qi, Y. Ji and M. Feng, *Int. J. Mech. Sci.*, 2023, **238**, 107828; https://doi.org/10.1016/j.ijmecsci.2022.107828.
81 S. Shuang, S. Lu, B. Zhang, C. Bao, Q. Kan, G. Kang and X. Zhang, *Comput. Mater. Sci.*, 2021, **195**, 110495; https://doi.org/10.1016/j.commatsci.2021.110495.
82 D. Ma, B. Grabowski, F. Körmann, J. Neugebauer and D. Raabe, *Acta Mater.*, 2015, **100**, 90; https://doi.org/10.1016/j.actamat.2015.08.050.
83 B. Song, Y. Yang, M. Rabbani, T. T. Yang, K. He, X. Hu, Y. Yuan, P. Ghildiyal, V. P. Dravid, M. R. Zachariah, W. A. Saidi, Y. Liu and R. Shahbazian-Yassar, *ACS Nano*, 2020, **14**, 15131; https://doi.org/10.1021/acsnano.0c05250.
84 Z. Sun, C. Shi, L. Gao, S. Lin and W. Li, *J. Alloys Compd.*, 2022, **901**, 163554; https://doi.org/10.1016/j.jallcom.2021.163554.

85 D. M. Duffy and A. M. Rutherford, *J. Phys.: Condens. Matter*, 2006, **19**, 016207; https://doi.org/10.1088/0953-8984/19/1/016207.
86 Q. Zeng, B. Chen, S. Zhang, D. Kang, H. Wang, X. Yu and J. Dai, *npj Comput. Mater.*, 2023, **9**, 213; https://doi.org/10.1038/s41524-023-01168-4.
87 J. Zeng, D. Zhang, D. Lu, P. Mo, Z. Li, Y. Chen, M. Rynik, L. Huang, Z. Li, S. Shi, Y. Wang, H. Ye, P. Tuo, J. Yang, Y. Ding, Y. Li, D. Tisi, Q. Zeng, H. Bao, Y. Xia, J. Huang, K. Muraoka, Y. Wang, J. Chang, F. Yuan, S. L. Bore, C. Cai, Y. Lin, B. Wang, J. Xu, J.-X. Zhu, C. Luo, Y. Zhang, R. E. A. Goodall, W. Liang, A. K. Singh, S. Yao, J. Zhang, R. Wentzcovitch, J. Han, J. Liu, W. Jia, D. M. York, W. E, R. Car, L. Zhang and H. Wang, *J. Chem. Phys.*, 2023, **159**, 054801; https://doi.org/10.1063/5.0155600.
88 C. Chen and S. P. Ong, *Nat. Comput. Sci.*, 2022, **2**, 718; https://doi.org/10.1038/s43588-022-00349-3.
89 B. Deng, P. Zhong, K. Jun, J. Riebesell, K. Han, C. J. Bartel and G. Ceder, *Nature Machine Intelligence*, 2023, **5**, 1031; https://doi.org/10.1038/s42256-023-00716-3.
90 A. Merchant, S. Batzner, S. S. Schoenholz, M. Aykol, G. Cheon and E. D. Cubuk, *Nature*, 2023, **624**, 80; https://doi.org/10.1038/s41586-023-06735-9.

Received: 5th February 2025; Com. 25/7742